# Feedback Acoustic Noise Control with Faust on FPGA: Application to Noise Reduction in Headphones

Loïc Alexandre, Pierre Lecomte, Marie-Annick Galland, Maxime Popoff

# FEEDBACK ACOUSTIC NOISE CONTROL WITH FAUST ON FPGA : APPLICATION TO NOISE REDUCTION IN HEADPHONES

*Loïc Alexandre*

LMFA, UMR5509
Univ Lyon, Ecole Centrale de Lyon, CNRS, Univ Claude Bernard Lyon 1, INSA Lyon, 69130, Ecully, France
loic.alexandre@ec-lyon.fr

*Pierre Lecomte*

LMFA, UMR5509
Univ Lyon, INSA Lyon, CNRS, Ecole Centrale de Lyon, Univ Claude Bernard Lyon 1, 69621, Villeurbanne France
pierre.lecomte@univ-lyon1.fr

*Marie-Annick Galland*

LMFA, UMR5509
Univ Lyon, Ecole Centrale de Lyon, CNRS, Univ Claude Bernard Lyon 1, INSA Lyon, 69130, Ecully, France
marie-annick.galland@ec-lyon.fr

*Maxime Popoff*

CITI, EA3720
Univ Lyon, INSA Lyon, Inria, 69621 Villeurbanne, France
maxime.popoff@insa-lyon.fr

## ABSTRACT

This work studies the feedback Active Noise Control (ANC) in a headphone with a digital filter implemented on a FPGA instead of an analog filter, in the context of a pedagogical practice bench. The digital approach allows greater flexibility in setting the feedback ANC filter but brings an additional latency that can compromise the ANC efficiency. The principle of feedback ANC in headphones is reviewed and the choice of a biquadratic filter as a feedback ANC filter is argued. The digital filter is programmed in the FAUST language and compiled on a FPGA platform. An experimental validation is carried out to compare the attenuation performance between the digital and analog biquadratic filters. The results show similar or even better low frequency attenuation for some configurations of the digital biquadratic filter compared to the analog filter. Finally, a digital filter cascading two biquads is studied and shows a bandwidth broadening where the ANC is effective.

## 1. INTRODUCTION

Active Noise Control (ANC) is an established solution for noise reduction in a large variety of applications [1]. In the case of headphones, ANC has become a technological and commercial asset by providing noise reduction in the low frequency band where the passive solution performs poorly. Based on the superposition of an external annoying sound with an "anti-sound", different approaches are possible to process the incoming unwanted sound and generate, in real-time, the canceling filtered sound. The main differences result from the ANC filter, referred to as the control filter throughout this paper. One of the first techniques described in the literature is the feedback approach. The sound and anti-sound signals are measured in the vicinity of the control region and fed back to the active noise control loudspeaker after passing through an ANC feedback control filter. The early implementation uses an analog filter as the control filter [2]. On one hand, the low-latency characteristics of the analog filter allows the control loop to generate the canceling sound instantly. On the other hand, the characteristics of the analog filter are fixed and the controlled frequency band cannot be adapted. Nowadays, the improved performance and the accessibility to low cost Digital Signal Processing (DSP) boards offer the opportunity to implement adaptive filtering algorithms in ANC headphone systems [3, 4]. However, with digital filtering appears the issue of latency due to Analog to Digital Converter (ADC) and Digital to Analog Converter (DAC). A solution to keep the convenience of programmable boards without obtaining unreasonable processing latency is the use of Field Programmable Gate Arrays (FPGAs) [5]. Based on configurable logic blocks, their basic architecture makes them faster than DSP boards and allows complex filtering configurations [6]. Unfortunately, the FPGAs' architecture also complicates significantly their programming.

In this context, the Fast Audio Signal-processing Technologies on FPGA [1] (FAST) project aims to simplify the FPGA programming by offering the compilation of FAUST algorithms onto FPGA boards [7]. The FAST programming tool is used in this paper in an academic context. Indeed, the authors' university proposes a training course on ANC in which an educational bench dedicated to the study of feedback ANC in headphones is used. The educational bench is shown in Fig. 1. The feedback ANC is currently operated using an analog biquadratic (biquad) filter with pre-set and fixed parameters : the box on the shelve on bottom left part of Fig. 1. The goal of this work is to replace this analog filter by a programmable digital biquad filter on FPGA with very low latency : the electronic boards on the middle of the table in Fig. 1. The FPGA circuit is synthesized from a FAUST code using the tool described in [7]. This implementation is considered more flexible as the digital filter parameters can easily be changed, which serves the educational purpose of the bench.

The outline of the paper is as follows: In Sec. 2 the principle of feedback ANC is reviewed. In particular, the specification of the feedback control filters is presented in Sec. 2.1 and the choice of a biquadratic control filter is argued in Sec. 2.2. The implementation on a FPGA board with FAUST is introduced in Sec. 3. An experimental validation of the proposed implementation is described in Sec. 4 and discussed in Sec. 5, especially in comparison with the current analog system used on the educational bench. Finally, the paper concludes in Sec 6.

[1] https://fast.grame.fr/

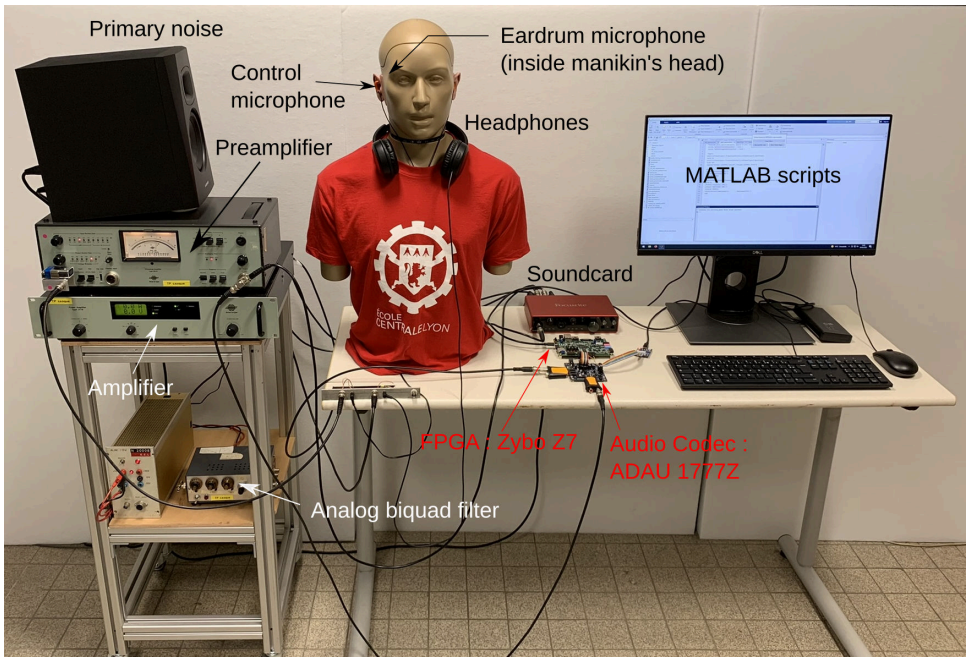


Figure 1: *Experimental set-up of the feedback ANC bench at Ecole Centrale Lyon. The set-up allows to study feedback ANC in headphones for academic purpose. The measurements are performed using ®MATLAB, an external soundcard and a loudspeaker for primary noise generation. The amplified headphones are placed on a head and torso simulator with eardrum microphone and a preamplified error microphone placed in its ear. An analog biquadratic filter is used as a control filter. In the current work, a digital biquadratic filter programmed on a FPGA board with external audio codec can be used as control filter for the feedback ANC.*

## 2. FEEDBACK ACTIVE NOISE CONTROL

### 2.1. Feedback with a Control Filter

This section describes the principle of the feedback ANC in headphones with a control filter as studied in [2]. The principle is depicted in Fig. 2 : a primary noise induces a pressure $p_p$ at a control microphone placed inside a headset. A secondary noise is generated by the headset speaker and induces a pressure $p_s$ at the control microphone. Therefore, the total pressure at the control microphone is given by $p_t = p_p + p_s$. The active noise control principle is to generate $p_s$, using a control filter $H$ and a gain $G$ to attenuate the total pressure $p_t$ with respect to $p_p$. The control microphone is placed close enough to the listener's eardrum so that the pressure at the latter is assumed to be equal to that at the control microphone. Thus, as $p_t$ decreases, the listener feels an attenuation of the noise from the primary source. The attenuation level and bandwidth depends on the ANC efficiency.

**Attenuation** The total pressure at the control microphone is given in the frequency domain by:

$$p_t(f) = p_p(f) + p_s(f) = p_p(f) + p_t(f)H(f)GB(f), \quad (1)$$

where $f$ is the frequency in Hz, $H(f)$ is the control filter Frequency Response Function (FRF), $G$ a frequency-independent gain and $B(f)$ the open loop FRF between the headphone speaker and the control microphone. From Eq. (1), for $p_p(f) \neq 0$, the attenuation can be written as:

$$\frac{p_t}{p_p}(f) = \frac{1}{1 - H(f)GB(f)} \quad (2)$$

Thus, in order to minimize the ratio $|\frac{p_t}{p_p}|$ the denominator in the right-hand side of Eq. (2) should be maximized. An attenuation occurs when $|H(f)GB(f)| \gg 1$. The greater the $|H(f)GB(f)|$ the greater the attenuation. As $B(f)$ is fixed from the headphone configuration, the role of $H(f)G$ is to increase the gain of the closed loop $H(f)GB(f)$ in the frequency range where attenuation is desired. However, when increasing the gain, the system stability must be considered. In fact, instability occurs with an audio feedback when $H(f)GB(f) = 1$.

**Control loop with a gain $G$** To better understand the requirements of control filter $H(f)$ and gain $G$ for an effective attenuation, the situation where $H(f) = 1$ is first considered. A typical FRF $GB(f)$ is shown in Fig. 3. The active attenuation is desired in the low frequency range where the passive attenuation of the headphone is poor.

When one increases the gain $G$, the modulus response $|GB(f)|$ is shifted upwards. Therefore, from Eq. (2) the noise at frequencies such that $|H(f)GB(f)| \gg 1$ will be attenuated. However, in the reported case of Fig. 3, it can be observed that the phase response $\arg(GB(f))$ crosses $0°$ around $f_{0°} = 5169$ Hz. At this value, the transfer function is real, and if the gain $G$ increases such that the modulus at 5169 Hz crosses 0 dB, one obtains, $|GB(f_{0°})| = 1$. The system becomes unstable. Moreover, the gain margin of 2.2 dB before instability, is not sufficient to verify the condition $|H(f)GB(f)| \gg 1$ in the low frequency region, where the atten-

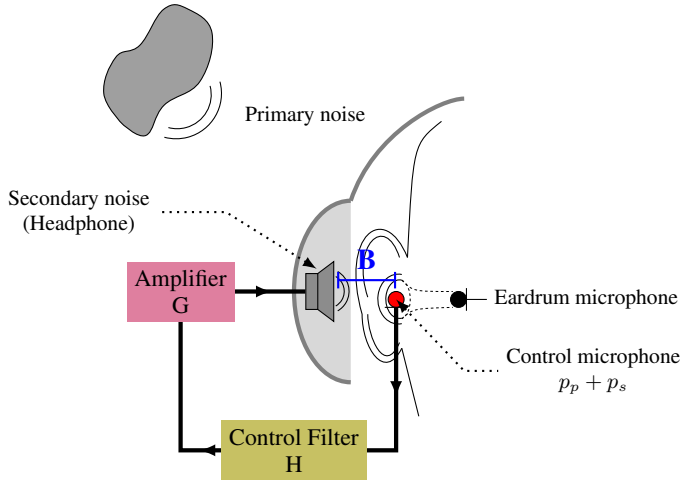


Figure 2: *Feedback ANC using a control loop with headphones: a control microphone is placed close to the eardrum in the headphone cavity. This microphone receives a pressure from a primary noise $p_p$ and a secondary noise $p_s$ from the headphone's speaker. With a control loop composed of a filter $H$ and an amplifier $G$, the pressure level from the external primary noise is attenuated at the control microphone and at the eardrum in its vicinity.*

uation is desired. In this case one cannot have attenuation without instability. A control filter is thus introduced to achieve an efficient noise reduction system.

**Control filter $H(f)$ requirements** The control filter should increase the modulus of $|GB(f)|$ FRF as much as possible with respect to $f_{0^\circ}$. The low frequency region of the spectrum is targeted, between $f_1$ and $f_2$. Thus, the control filter $H(f)$ should be such that $\forall f \in [f_1, f_2]$:

$$|H(f)GB(f)| \gg 1 \text{ AND } \arg(H(f)GB(f)) \neq 0. \quad (3)$$

### 2.2. Biquadratic Transfer Function as Control Filter $H(f)$

An ideal solution for $H(f)$ to achieve Eq. (3) is $-B^{-1}(f)$. However, the latter is not causal and therefore cannot be implemented [2]. In the pedagogical bench context, a biquadratic filter [8] is used for $H(f)$ by using two resonant filters: a filter with a pair of complex conjugate zeros[2], and a filter with a pair of complex conjugate poles[3]. This choice is justified by the fact that the phase response can be set such that it does not change that of $\arg(GB(f))$ around $f_{0^\circ}$. The biquadratic analog transfer function is given by:

$$H(s) = \frac{s^2 + 4\pi f_z \xi_z s + (2\pi f_z)^2}{s^2 + 4\pi f_p \xi_p s + (2\pi f_p)^2}, \quad (4)$$

where $s$ is the Laplace's variable, $f_z$ and $f_p$ are the resonant frequencies of the two zeros and two poles filters respectively. $\xi_z$ and $\xi_p$ are the damping factors of the two-zero and two-pole filters respectively.

[2] `https://ccrma.stanford.edu/~jos/fp/Two_Zero.html`

[3] `https://ccrma.stanford.edu/~jos/fp/Two_Pole.html`

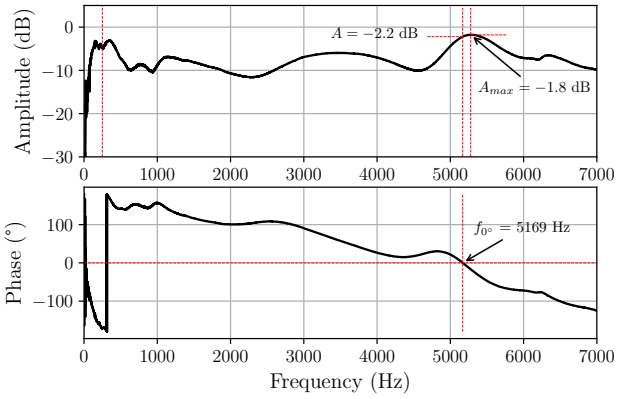


Figure 3: *Modulus (top graph) and phase (bottom graph) response of the transfer function $GB(f)$ between the amplifier and the control microphone. The FRF is measured in the experiment described in Sec. 4. The phase response crosses $0^\circ$ at $f_{0^\circ} = 5169$ Hz. At this frequency the modulus is $A = -2.2$ dB. The maximum amplitude is at $f = 5278$ Hz at $A_{max} = -1.8$ dB.*

**Two-pole filter** The two-pole filters allow to reinforce a frequency band by adjusting the resonance frequency $f_p$ and the damping factor $\xi_p$. The resonance can be set, for example, to a maximum of $|GB(f)|$ spectrum, in the low frequency region before $f_{0^\circ}$. For instance, from Fig. 3 one can choose $f_p = 250$ Hz. The dynamic range available for attenuation at this frequency before the instability occurs is then increased, as discussed in Sec. 2. Another strategy is to adjust the resonance frequency $f_p$ to boost another zone of the low frequency region of $|GB(f)|$ spectrum. This will improve the attenuation at this frequency and broaden the frequency band where attenuation is possible. However, this strategy will provide less dynamic range compared to a situation where the resonance would be placed on a maximum. Thus, a compromise between bandwidth and dynamic attenuation should be made by the user when setting the parameters $f_p$ and $\xi_p$.

**Phase response** A two-pole filter rotates the phase by $-90^\circ$ after the resonance frequency $f_p$. The transition zone between $0^\circ$ and $-90^\circ$ depends on the value of $\xi_p$. Thus, if one were to use only a two-pole filter, $\arg(GB(f))$ would cross $0^\circ$ at a lower frequency in the spectrum, which is not desirable as this limits the bandwidth of the possible attenuation. The use of a two-zero filter allows to overcome this problem. Indeed, the latter rotates the phase by $+90^\circ$ after the resonance frequency $f_z$. Thus, by placing the resonance frequency $f_z$ close to $f_p$ and by tuning the values of $\xi_p$ and $\xi_z$, the use of the biquadratic filter does not change the value of $f_{0^\circ}$. This type of filter thus makes it possible to answer to a certain extent the criterion of Eq (3).

**Analog and digital biquad filters** Three examples of biquadratic FRF are shown in Fig. 4. The resulting FRF of the control loop $H(f)GB(f)$ are shown in Fig. 5.

The black solid line corresponds to the response of the analog biquad filter cell of the educational bench. The phase response $\arg(H_a(f))$ is almost null except in the vicinity of the resonances frequencies $f_p$ and $f_z$ of the poles and zeros pair respectively. In

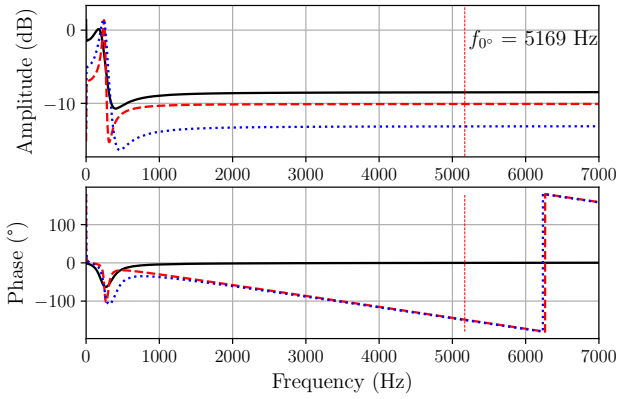


Figure 4: *Modulus (top graph) and phase (bottom graph) response of biquadratic filters transfer functions. Black solid line: $H_a(f)$ analog biquad filter of the educational bench (see Fig. 1). Red dashed line $H_{d1}(f)$ and blue dotted line $H_{d2}(f)$ : two realizations of digital biquad filters on FPGA Zybo Z7 + ADAU 1777Z audio codec. The digital filters parameters for $H_{d1}(f)$ are: $f_p = 250$ Hz, $f_z = 300$ Hz, $\xi_p = 0.07$, $\xi_z = 0.1$ and for $H_{d2}(f)$: $f_p = 250$ Hz, $f_z = 400$ Hz, $\xi_p = 0.16$, $\xi_z = 0.25$. Frequency where the phase response crosses 0 ($f_0$) is indicated with a vertical dashed line.*

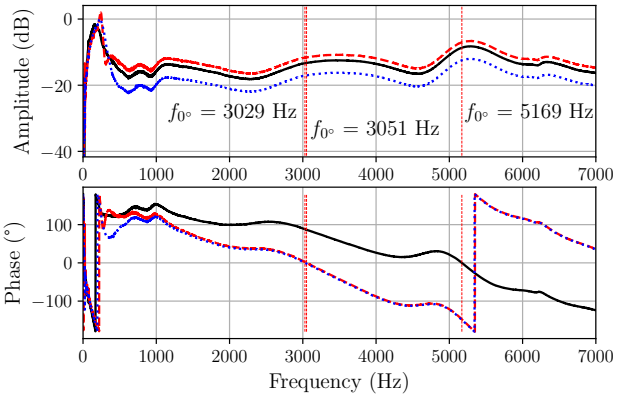


Figure 5: *Modulus (top graph) and phase (bottom graph) response of closed-loop transfer function $H(f)GB(f)$. Black solid line: $H_a(f)GB(f)$. Red dashed line $H_{d1}(f)GB(f)$ and blue dotted line $H_{d2}GB(f)$. Frequency where the phase response crosses 0 ($f_0$) is indicated with a vertical dashed line.*

particular, the fact that the filter is analog results in an almost null group delay, which does not modify $f_{0^\circ}$ of $GB(f)$ and therefore does not change the ANC theoretical bandwidth.

The red dashed and blue dotted curves correspond to two digital realizations of the biquad filter with slightly different parameters. In comparison with the analog filter, one can see a slope in the phase response $\arg(H_{d1}(f))$ and $\arg(H_{d2}(f))$. This constant group delay is due to the latency the ADC and DAC of the audio codec .

Thus, the phase slope of $\arg(H_{d1,2}(f))$ impacts the phase response of $\arg(H_{d1,2}(f)GB(f))$ and decreases the value of $f_{0^\circ}$ as it can be seen in Fig. 5. The $f_{0^\circ}$ frequencies are respectively 3029 Hz and 3051 Hz for the digital filters presented compared to 5169 Hz for the analog filter. The ANC bandwidth is therefore reduced in this case. A theoretical analysis taking into account sine signals and a system with a flat frequency response, as in [4, Sec. 3.2], suggests that a digital filter with the lowest possible latency is desirable for feedback ANC. However, while the ANC bandwidth narrows as the latency increases, the achievable attenuation in the given frequency bandwidth is also highly dependent on the system frequency response. In the case of the FRF $GB(f)$ considered here, the shift of the unstable frequency due to the latency leads to a higher dynamic for attenuation in the low frequency region. Indeed, the amplitude of $GB(f)$ being lower at the shifted unstable frequency, the amplitude margin before instability is greater. This allows to further increase the gain $G$ and therefore improves the attenuation. The topic of latency effect on ANC performance is left for further investigations.

In the three cases, the control filter $B(f)$ allows to raise the low frequency region of the spectrum $H(f)GB(f)$ below the instability and improves the attenuation dynamic according to Eqs. (2) and (3). It should be kept in mind that the digital filters can be adjusted online and that the passive attenuation of the headphones also helps in the high frequency region.

## 3. IMPLEMENTATION WITH FAUST ON FPGA

As discussed in Sec. 2.2, the control filter $H(f)$ for this work is a biquad filter. Its implementation on the FPGA is done using the workflow proposed in [7]. The FPGA evaluation board Zybo Z7 is used for this work alongside an audio codec ADAU1777Z. The latter has a round trip latency around 80 $\mu$s at a sampling frequency of 192 KHz.

**Single biquad implementation** The biquad transfer function is directly taken from Eq. (4) in the analog domain and transformed into a digital filter by a bilinear transform [9, Sec. 7.2]. This operation is performed using the function `tf2s` from the library `filters.lib` from the FAUST distribution. The resulting code is given hereafter:

```
import("stdfaust.lib");

fp = hslider("Freq Pole",150,50,1000,0.1);
fz = hslider("Freq Zero",150,50,1000,0.1);
xip = hslider("Tau Pole",0.1,0,1,0.01);
xiz = hslider("Tau Zero",0.1,0,1,0.01);

b1 = 4 * ma.PI * fz * xiz;
b0 = (2 * ma.PI * fz)^2;

a1 = 4 * ma.PI * fp * xip;
a0 = (2 * ma.PI * fp)^2;

w1 = 1;
// w1 is the desired digital frequency
//(in radians/second) corresponding to the
//analog frequency 1 rad/sec (i.e., s = j).

process = _ : fi.tf2s(1,b1,b0,a1,a0,w1);
```

Note that the user can control at execution time the resonant frequency of the pole $f_p$ and the zero $f_z$, as well as their respective damping rates $\xi_p$ and $\xi_z$ using a user interface generated on the computer or with a hardware board as presented in [7].

**Cascaded biquad implementation** In order to improve the ANC bandwidth as discussed in Sec. 2, another version of the $H(f)$ control filter is implemented as a cascade of two biquads. In this case, the user can control the parameters of each of the biquad sections of the filter and activate or bypass them using a checkbox. The FAUST code is the following:

```
import("stdfaust.lib");

fp(i) = hslider("[1]Freq Pole %i
    ",150,50,1000,0.1);
fz(i) = hslider("[3]Freq Zero %i
    ",150,50,1000,0.1);
xip(i) = hslider("[2]Tau Pole %i
    ",0.1,0,1,0.01);
xiz(i) = hslider("[4]Tau Zero %i
    ",0.1,0,1,0.01);

off(i) = 1-checkbox("[5]Off %i");

b1(i) = 4 * ma.PI * fz(i) * tz(i) * off(i
    );
b0(i) = (2 * ma.PI * fz(i))^2 * off(i);

a1(i) = 4 * ma.PI * fp(i) * tp(i) * off(i
    );
a0(i) = (2 * ma.PI * fp(i))^2 * off(i);

w1 = 1;

process = _ : seq(i, 2, fi.tf2s(1,b1(i),
    b0(i),a1(i),a0(i),w1));
```

## 4. EXPERIMENTAL VALIDATION

**Experimental layout** The experimental layout is visible in Fig. 1. An instrumented dummy head (®G.R.A.S Kemar 45BB head and torso simulator) is used. Only the right-ear is used for the practical. The feedback control loop ($H(f)GB(f)$) is composed of a ®JVC HA-S31M-B headphones for which the input signal is amplified by a ®B&K Type 2718 power amplifier ($G$). The control microphone inside the loop is a standard electret microphone placed in a 3D printed support [4]. Its output signal is preamplified by a ®B&K Type 2610 preamplifier with fixed gain and goes to the feedback loop biquad filter which is either:

- An analog biquad filter, $H_a(f)$, as visible on the lower shelf on the bottom left side of Fig. 1,
- A digital biquad filter, $H_d(f)$ implemented on a ®Xilinx ZYBO Z7 FPGA evaluation board alongside an ADAU 1777Z audio codec.

The primary noise source uses a low-pass filtered white noise played on a ®Adam Audio T5V loudspeaker.

[4] http://sekisushai.net/ambitools/2020/12/02/make-your-own-binaural-microphones.html

Acquisition and primary noise signal generation are performed by a ®Focusrite Scarlett 8i6 3rd Gen soundcard. FRF measurement and spectrum displays are done with ®MATLAB scripts.

The sound pressure level of the noise produced by the external loudspeaker is about 70.6 dBA at the exterior of the manikin ear.

**Protocol** The experimental protocol consists in measuring first the FRF $GB(f)$. Its analysis allows to identify the frequency band for which ANC is possible, in particular to determine $f_{0^\circ}$ as described in Sec.2. Then, the biquadratic control filter $H(f)$ is designed in adequacy. Although many solutions exist to choose the poles' and zeros' characteristics of the control filter [6], the method adopted here is empirical with the intention of observing the impact of the biquad parameters on the sound pressure level attenuation. Therefore, the filter parameters $f_p, f_z, \xi_p$ and $\xi_z$ are set manually from the analysis of FRF $GB(f)$. Once $H(f)$ parameters are set, the transfer function $H(f)GB(f)$ is deduced and can be also measured to predict the ANC performance. Finally, the ANC performance is measured as follows: A primary noise is played in the frequency band [50-1000] Hz through the external loudspeaker and the gain $G$ is increased until the audio feedback is observed. Finally, with the gain set to its maximum value, the measurement of the eardrum microphone signal is carried out with and without the headphones feedback ANC system. The difference between the two measurements gives the attenuation as a function of the frequency performed by the ANC feedback system.

## 5. RESULTS AND DISCUSSION

This section presents the results obtained for several control filter configurations. The reference configuration is the analog biquad filter $H_a(f)$ visible as solid line in Fig. 4 and its corresponding closed loop transfer function in Fig. 5.

### 5.1. Single Biquad Configuration

The FRF $H_{d1}(f)$ of the first digital control filter and the corresponding configuration are presented in Figs. 4 and 5 with a red dashed line. As explained in Sec. 2.2, the digital filter latency reduces $f_{0^\circ} = 5169$ Hz to $f_{0^\circ} = 3051$ Hz in comparison with the analog filter $H_a(f)$. However, as the primary noise is in the range $[50 - 1000]$ Hz, this bandwidth limitation is not relevant here and the filter $H_{d1}(f)$ can be used for feedback ANC.

One of the main advantage of the digital control filter implementation is the configuration flexibility : as explained in Sec. 3, a user interface allows modifying the filter parameters in real-time. In this matter, a second digital control filter configuration, $H_{d2}(f)$ is presented with a blue dotted line in Figs. 4 and 5.

The ANC attenuation is shown in Fig. 6 using either the $H_a(f)$ (black solid curve), $H_{d1}(f)$ (red dashed curve) or $H_{d2}$ (blue dotted curve) as control filter. It corresponds to the ratio of pressure measured at the eardrum microphone without ANC and with ANC. It can be observed that the higher attenuation is concentrated in the frequency range [50-400] Hz, which is in accordance to the control filter configurations. It is consistent that with a single biquad filter, the frequency range operation of the ANC is limited. In the case of the analog control filter $H_a(f)$ the attenuation obtained is above 10 dB in a narrow frequency band from 154 Hz to 195 Hz. For the first digital control filter $H_{d1}(f)$, the attenuation reaches 10 dB with a maximum at 15.4 dB in the frequency region [158-261] Hz. One may observe the important peak

of attenuation due to the low damping poles and zeros coefficients chosen for this configuration. Finally, the third filter $H_{d2}(f)$ gives the most interesting results with an attenuation above 10 dB over the frequency band [102-297] Hz and with a maximum attenuation reaching 19.4 dB. This comparison of the analog filter configuration with two different digital filter configuration does not only aim to validate the employment of digital control filters but also to demonstrate the importance of configuration flexibility. As a matter of fact, if for a single biquad filter the chosen configuration can severely change the obtained noise attenuation, the design must be wisely chosen for a more complex filter.

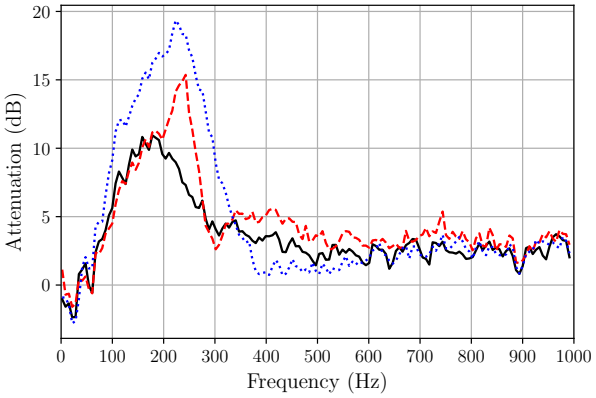


Figure 6: *Noise attenuation obtained with three different control filters $H(f)$. Black solid line: $H_a$. Red dashed line $H_{d1}$ and blue dotted line $H_{d2}$.*

### 5.2. Cascade Configuration of Biquad Filters

As an extension to the reference single analog control filter, this section presents a configuration with two cascade digital biquad filters whose implementation is presented in Sec. 3.

Two configurations, $H_{d3}(f)$ and $H_{d4}(f)$ are evaluated. Their frequency response and resulting closed loop FRF $H(f)GB(f)$ are shown in Figs 7 and 8 respectively. As for the previous case with a single biquad filter, the two cascade configurations lower the frequency of instability of the closed loop. In comparison with the analog filter $H_a(f)$, $f_{0^\circ} = 5169$ Hz is shifted to $f_{0^\circ} = 2886$ Hz with $H_{d3}(f)$ and to $f_{0^\circ} = 2813$ Hz with $H_{d4}(f)$. Although the resulting frequencies of instability are much lower than the initial one, noise attenuation is still achievable in the bandwith of interest [50-1000] Hz. The setting differences between both configurations relies exclusively on the damping coefficients of the complex conjugate poles and zeros. In fact, the cascade of biquad filters $H_{d4}(f)$ is smoother, which means that the damping coefficients are higher, than the first cascade $H_{d3}(f)$. Because of the more complex filter configuration the effective frequency range of attenuation is wider than for the previous case using only a single biquad filter. The results of noise attenuation are presented in Fig. 9. In the case of the first cascade biquad filters $H_{d3}(f)$ (black solid line) the noise attenuation obtained is equal or superior to 10 dB in the frequency band [80-498] Hz with a maximum attenuation at 22 dB. Addtionally, the attenuation reaches 15 dB or more over a quite large frequency region, from 101 Hz to 466 Hz. Concerning the second cascade biquad filters $H_{d4}(f)$ (red dashed line), the attenuation reaches 10 dB and above in the bandwidth [82-546] Hz. For the threshold of 15 dB, an attenuation is obtained in the frequency band [135-483] Hz and the maximum attenuation is 21.3 dB. One can notice that the shape of the attenuation is actually similar to the shape of the corresponding cascade of biquad filters. This behavior is in line with the aim to design a control filter with amplitude resonances in the bandwith requiring noise attenuation. The design of the two biquad filters in $H_{d3}(f)$ helps to obtain these two peaks of attenuation around 160 Hz and 415 Hz. Therefore, one must modify the design of the control filter depending on the desired outcome. A further investigation on the addition of an optimization method to design the control filter is a perspective to this study.

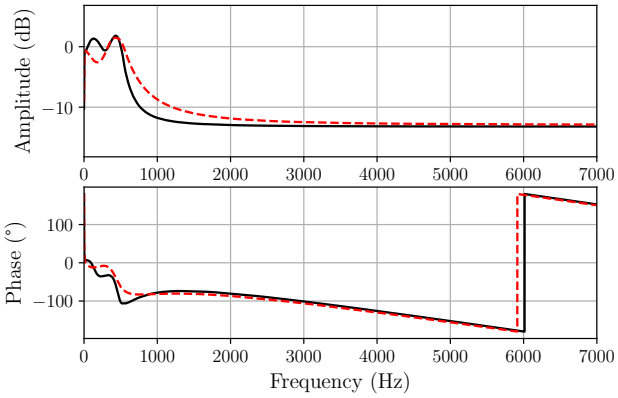


Figure 7: *Modulus (top graph) and phase (bottom graph) FRF of biquadratic filters. Black solid line: $H_{d3}(f)$ the control filter composed of two cascaded biquads with parameters : $f_{p1} = 150$ Hz, $f_{z1} = 250$ Hz, $\xi_{p1} = 0.5$, $\xi_{z1} = 1$, $f_{p2} = 450$ Hz, $f_{z2} = 550$ Hz, $\xi_{p2} = 0.125$, $\xi_{z2} = 0.5$. Red dashed line: $H_{d4}(f)$ the control filter composed of two cascaded biquads with parameters : $f_{p1} = 150$ Hz, $f_{z1} = 250$ Hz, $\xi_{p1} = 1$, $\xi_{z1} = 1$, $f_{p2} = 450$ Hz, $f_{z2} = 550$ Hz, $\xi_{p2} = 0.25$, $\xi_{z2} = 1$.*

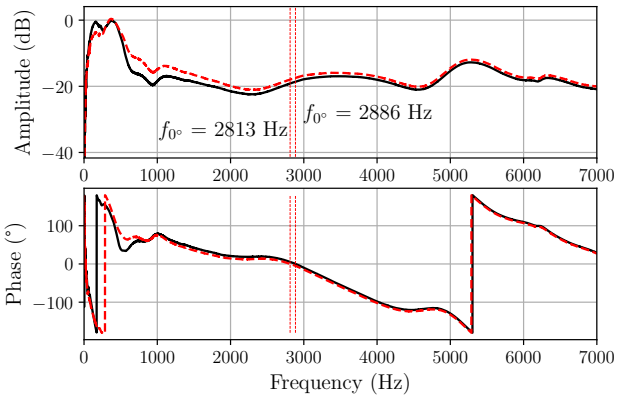


Figure 8: *Modulus (top graph) and phase (bottom graph) response of closed-loop transfer function $H(f)GB(f)$. Black solid line: $H_{d3}(f)GB(f)$ and red dashed line $H_{d4}(f)GB(f)$.*

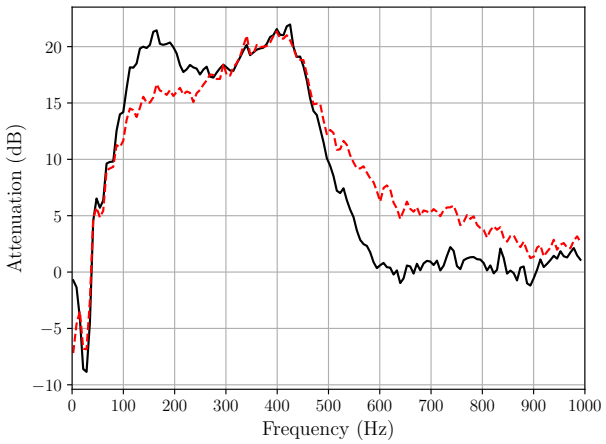


Figure 9: *Noise attenuation obtained with two different control filters $H(f)$. Black solid line: $H_{d3}(f)$ and red dashed line $H_{d4}(f)$.*

## 6. CONCLUSION

In this paper, the comparison between an analog and digital filters for feedback ANC in headphones was studied in the context of a pedagogical bench. The principle of feedback ANC in headphones was reviewed and the choice of a biquadratic filter as a control filter was argued. Then, the process to implement the desired control filter with FAUST was explained both for single and cascade biquad filter configurations. Furthermore, an experimental approach was proposed to validate the use of a digital control filter through the evaluation of the noise attenuation performance. Therefore, the results were presented and discussed for two biquad filter designs per configuration. In particular, a single digital biquad configuration achieved an attenuation above 10 dB in the bandwidth [102-297] Hz while the attenuation achieved is superior to 15 dB, in the frequency range [101-466] Hz, using a cascade of two biquad filters. This work is based on an existing educational bench dedicated to feedback ANC headphones. While this experiment is initially using an analog biquad as control filter, the latter was successfully replaced with a digital filter programmed on a FPGA evaluation board. The aim is to offer a wider flexibility of parameterization for pedagogical aspects. The programming workflow using the FAUST programming language greatly simplify the digital filter implementation on FPGA. A systematic way of studying, modeling and realizing feedback active control systems has been outlined here. Future works include the study of latency effect on ANC performance as well as digital filter optimization with respect to the headphone to control microphone FRF.

## 7. ACKNOWLEDGMENTS

This work was supported by the French National Research Agency, ANR FAST (ANR-20-CE38-0001).

This work was carried out within the LABEX CeLyA (ANR-10-LABX-0060) of the University of Lyon.

## 8. REFERENCES

[1] Stephen J Elliott, *Signal Processing For Active Control*, Academic Press, London, 2001.

[2] C. Carme, "Absorption acoustique active dans les cavités auditives," *Acta Acustica united with Acustica*, vol. 66, no. 5, pp. 233–246, Oct. 1988.

[3] W.S. Gan, S. Mitra, and S.M. Kuo, "Adaptive feedback active noise control headset: implementation, evaluation and its extensions," *IEEE Transactions on Consumer Electronics*, vol. 51, no. 3, pp. 975–982, Aug. 2005, Conference Name: IEEE Transactions on Consumer Electronics.

[4] Stefan Liebich, Johannes Fabry, Peter Jax, and Peter Vary, "Signal processing challenges for active noise cancellation headphones," in *Speech Communication; 13th ITG-Symposium*. 2018, pp. 1–5, VDE.

[5] Piero Rivera Benois, Patrick Nowak, and Udo Zölzer, "Fully digital implementaiton of a hybrid feedback structure for broadband active noise control in headphones," 07 2017.

[6] Jiajie Wang, Jinhui Zhang, Jian Xu, Chengshi Zheng, and Xiaodong Li, "An optimization framework for designing robust cascade biquad feedback controllers on active noise cancellation headphones," *Applied Acoustics*, vol. 179, pp. 108081, Aug. 2021.

[7] Maxime Popoff, Romain Michon, Tanguy Risset, Yann Orlarey, and Stephane Letz, "Towards an FPGA-Based Compilation Flow for Ultra-Low Latency Audio Signal Processing," in *SMC*, Saint Étienne, 2022.

[8] Behzad Razavi, "The biquadratic filter [a circuit for all seasons]," *IEEE Solid-State Circuits Magazine*, vol. 10, no. 2, pp. 11–109, 2018.

[9] Alan V Oppenheim and Ronald W Schafer, *Discrete-Time Signal Processing*, Pearson Higher Education, Upper Saddle River, 3rd edition, 2010.